Experimental Study on Electrodeless Electromagnetic Acceleration in Helicon Plasma Thruster

IEPC-2013-112

D. Kuwahara, S. Waseda, H. Ishii, N. Teshigahara, H. Fujitsuka, T. Ishii,
S. Otsuka, T. Nakagawa, S. Shinohara
Tokyo University of Agriculture and Technology, Koganei, Tokyo, 184-8588, Japan

Abstract: To establish a completely electrodeless plasma thruster, we have been studying electromagnetic acceleration methods proposed and estimating plasma performance by the use of various diagnostics. Our experimental device LMD (Large Mirror Device) utilizes a radiofrequency source (7 MHz, ~ 5 kW) for producing a high-density helicon plasma. As well, we use both permanent magnets and electromagnets for generating large radial component of magnetic fields to increase an effect of electromagnetic acceleration by proposed methods of including azimuthal current. In this article, we present our ongoing research on helicon plasma thruster, especially focusing on thrust measurement system and its preliminary result.

Nomenclature

B_r	=	radial component of magnetic field
f_{rf}	=	excitation radio frequency for plasma production
F_z	=	axial component of Lorentz force
j_θ	=	azimuthal component of current in plasma
m	=	azimuthal mode number
m_i	=	mass of ion
m_n	=	mass of neutral particle
n_e	=	electron density
n_n	=	neutral particle density
P_{rf}	=	input power of radio frequency
r	=	plasma radius
T_n	=	neutral particle temperature
μ	=	magnetic moment
v_i	=	flow velocity of ion
v_n	=	flow velocity of neutral particle
ω_{ce}	=	electron cyclotron angular frequency
ω_{ci}	=	ion cyclotron angular frequency
λ	=	inverse of normalized skin depth
γ	=	Hall parameter

I.   Introduction

An electric thruster is an indispensable propulsion method for a long-time mission such as a deep space exploration due to a high specific impulse. However, electric thrusters, e.g., ion engine, Hall thruster and MPD thruster, have a problem of electrode erosion due to direct contact with plasmas. Therefore, to extend the lifetime of

a thruster, it is essential to eliminate electrodes contacting directly with plasmas. To solve this problem, we have been studying a helicon plasma thruster under the HEAT (Helicon Electrodeless Advanced Thruster) project.[1] Our object is to establish a method of a completely electrodeless electric thruster. The outline of the helicon plasma thruster proposed is as follows: First, to generate a dense source plasma using a helicon wave[2] with an excitation frequency between ion and electron cyclotron ones applied from an outside of a discharge cylinder (non-contact with plasma) using an antenna. Second, in order to yield a higher thrust, the dense plasma is accelerated by Lorentz force F_z with the product of the induced azimuthal current j_θ and the static radial magnetic field B_r. There are several methods proposed in our HEAT project of exciting j_θ in plasma, and our laboratory are promoting schemes by the use of two types of coils: Rotating Magnetic Field (RMF)[3] coils and an m (azimuthal mode number) = 0 coil.[1,4] Here, B_r is generated with a combination of permanent magnets, which have relatively larger B_r component, and electromagnets surrounding a discharge cylinder. We have succeeded in generating high-density (Ar, $> 3 \times 10^{12}$ cm^{-3}) plasmas on LMD (Large Mirror Device, Fig. 1),[5] and have observed the increases of the flow velocity and the electron density than using electromagnets alone.

In verifying our acceleration schemes, plasma diagnostics such as a plasma thrust, an ion flow velocity and density measurements in plasma are required. LMD can accept above-mentioned measurements, which will be described in detail later: The thrust measurement system uses a pendulum–type thrust stand with a cylindrical target.[6] Ion velocity is measured by three methods: a high-resolution spectrometer and directional electrostatic probes as well as a Laser Induced fluorescence (LIF) method.[7] In particular, LIF has an advantage in time and space resolution, and it can determine particle velocity and temperature absolutely. In addition, in order to obtain 2D profiles of plasma light emission during the acceleration phase, we have a high-speed camera (1024×1024 pixel, 1.3 MFPS, Photron, FASTCAM-SA5) with interference filters (Ar I and Ar II lines). By the use of this camera with perpendicular view optics, local neutral and electron densities are derived by an asymmetrical Abel inversion, ART (Algebraic Reconstruction Technique) and computational tomography method.[8, 9]

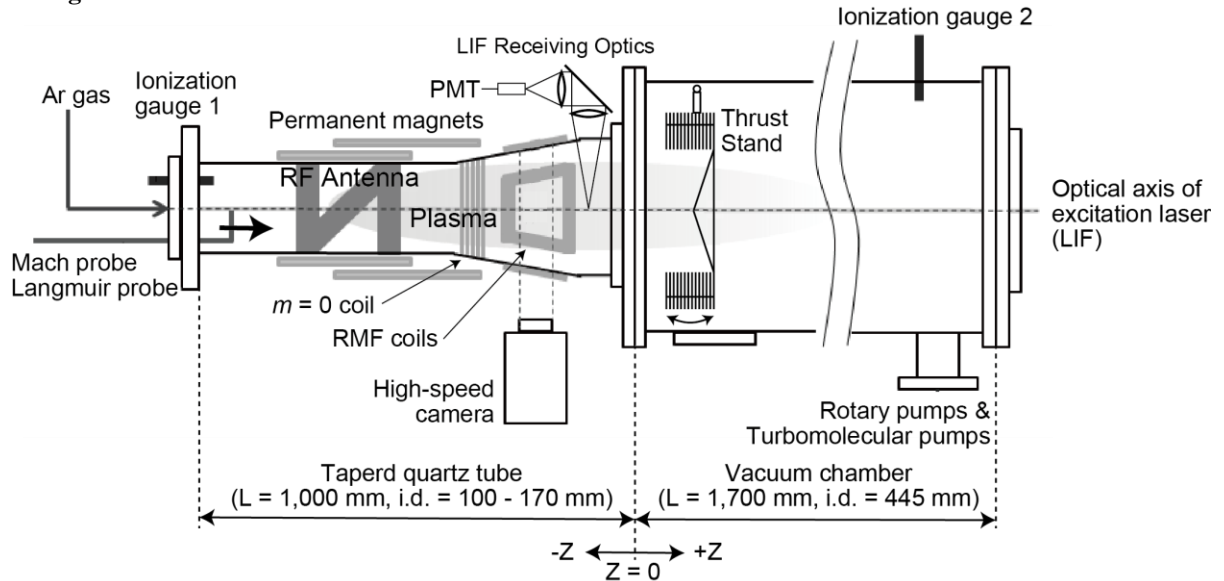## II. Experimental Apparatus

A. Large Mirror Device

Figure 1. Schematic of Large Mirror Device

Figure 1 shows a schematic diagram of LMD. Considering a divergent magnetic field to be applied in the acceleration scheme, a quartz tube (1,000 mm in length, 100~170 mm in inner diameter (i.d.)) has a tapered shape to prevent a wall loss of plasmas. LMD has two turbo-molecular pumps (1,000 l/s and 2,400 l/s) with a base pressure < 10^{-4} Pa. An argon gas is used as a propellant one, and a typical discharge pressure is ~ 0.1 Pa. A helicon plasma is generated by a radio frequency (rf) power via a half-helical antenna. The rf input power P_{rf} and its excitation frequency f_{rf} are ~ 3 kW and 7 MHz, respectively. An external magnetic field is applied by 12 sets of electromagnets.

In order to increase B_r, specialty designed permanent magnets were also installed. As to acceleration antennas, RMF and $m = 0$ coils are put on a tapered quartz tube position where the strong B_r is obtained. For plasma measurements, Langmuir probes and Mach probes are used to obtain electron density n_e and argon ion velocity v_i, respectively. Also optically measurement, such as spectroscopic method and LIF one are utilized as non-disturbance measurement. Here, typical values of LMD plasma are as follows. n_e: $10^{18} - 10^{19}$ m^{-3}, v_i: < 3 km/s, mass flow rate of Ar gas: 20 – 70 sccm.

B. Electromagnets and Permanent Magnets

In our proposed methods of the electrodeless acceleration, the high-density helicon plasma is accelerated by the Lorentz force, i.e., the product of the j_θ and B_r. However, the strength of B_r using the electromagnets is not strong enough to have the necessary propulsion. Therefore, the use of permanent magnet designed was proposed to increase B_r from a few tens of G to > 100 G, which is crucial for accelerating plasma by both RMF and $m = 0$ methods. Permanent magnets in addition to the present electromagnets were placed in a quartz tube straight section (see Fig. 2). Compared with the case using only electromagnets, an increase of ion velocity in the acceleration region was confirmed by the use of permanent magnets mainly due to the increased effect of -μ grad B force, where μ is a magnetic moment.
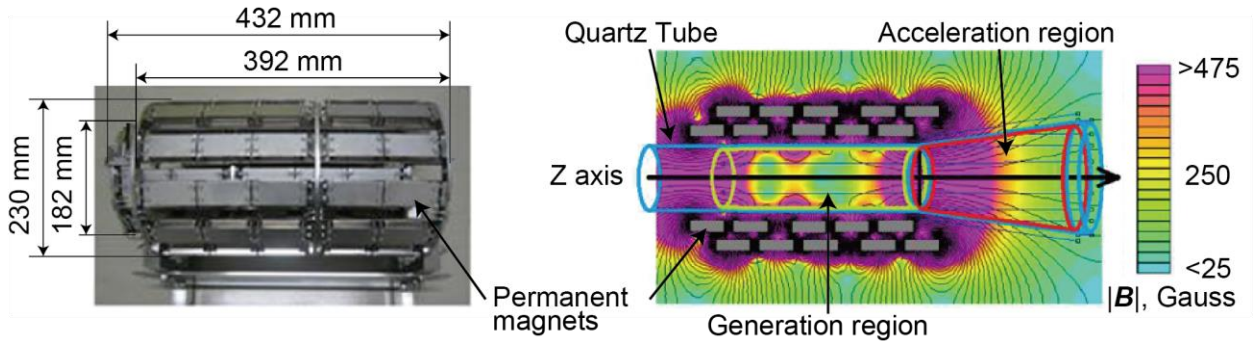

Figure 2. Permanent magnets and its magnetic field strength and lines

C. Electromagnetic Acceleration

Figure 3 shows the RMF acceleration scheme. RMF is generated by two opposing sets of currents, which have a phase difference of 90 degrees. If $\omega_{ci} < \omega < \omega_{ce}$, only electron can rotate, then j_θ can be generated. Here, ω_{ci} (ω_{ce}) is an ion (electron) cyclotron angular frequency and ω is an angular frequency of RMF. A penetration ratio of RMF into a plasma depends on two dimensionless parameters: normalized plasma radius λ and Hall parameter γ.[10] In order to check this, an experiment was done under a partial penetration condition (P_{rf} = 2,800 W, RMF = 2.5 G and RMF frequency = 1 MHz), and a radial distribution of RMF signal in plasma was measured by a magnetic probe. From the result, RMF penetrated into plasma fully, even the partial penetration condition is expected from a simulation. This result shows promising for our propulsion scheme and operating conditions can be extended.
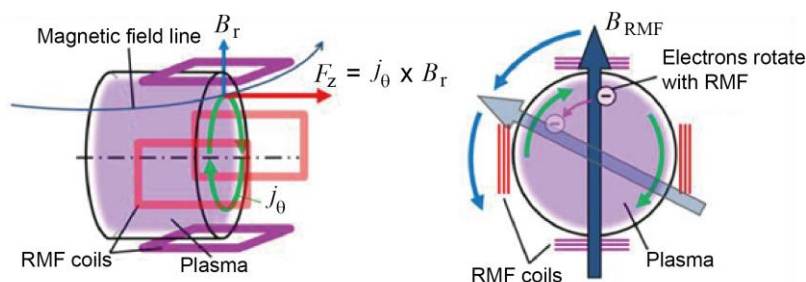

Figure 3. Acceleration principle with RMF coils.

The $m = 0$ coil acceleration is a half cyclic one by the use of a low frequency current near ω_{ci}. Figure 4 shows a conceptual diagram of this scheme. Conditions required for the acceleration are follows: 1) accelerated plasma needs an exhaust from the $m = 0$ antenna area before undergoes a deceleration phase, 2) an inductance of the plasma is

3

dominant than a resistance, 3) electric and magnetic fields generated by the $m = 0$ coil need to be penetrated into a plasma. Critical operating parameters to achieve an efficient acceleration condition is an external magnetic field strength, a driving frequency and magneto motive force of the $m = 0$ coil. Initial simulation done by K. P. Shamrai results showed an operation window in an ion cyclotron frequency range. Preliminary measurements show a change of Langmuir probe signal with $m = 0$ coil driving frequency.
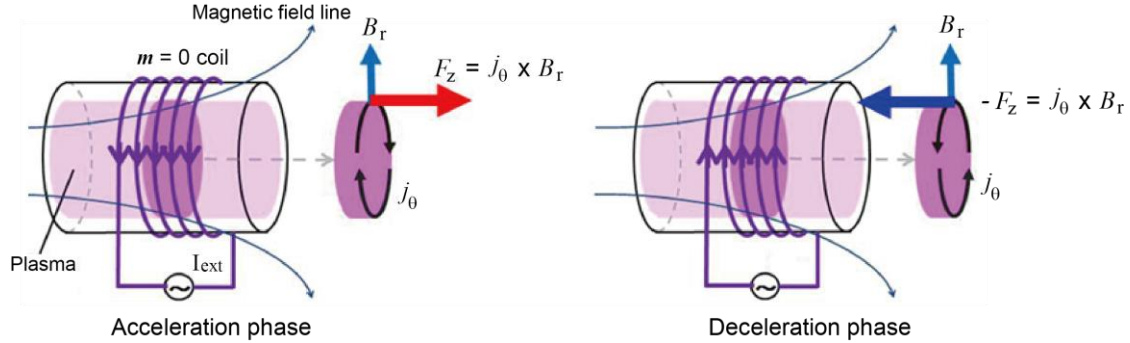

Figure 4. Acceleration principle with $m = 0$ coil.

D. Spectroscopy

In order to estimate an ion flow velocity and its temperature, we measured an ion Doppler shift and a broadening of emission spectrum by using a high-resolution spectrometer, Ritsu Ouyou Kougaku, Czerny-Turner type MC-150 (wavelength range: 190~600 nm, focal length of collimating lens: 1,500 nm, grating: 2,400 lines/mm, resolution: 0.006 nm). An accuracy of an ion flow velocity of ~ 0.5 km/s was obtained. We are developing a spectroscopic method of determining an electron density and its temperature from emission intensity ratio of ArI, based on a collisional-radiative model.[11]

E. Laser induced fluorescence

Since LIF is a powerful tool for plasma diagnostics, because of a non-invasive method with a high spatial resolution, it can deduce velocity distributions of any particles (ions, atoms and molecules). For an argon ion, we use a classical LIF scheme, in which Ar II $3d^4F_{7/2}$ metastable state is optically pumped by 668.16 nm (in vacuum) laser light to $4p^4D_{5/2}$ state, which decays to $4s^4P_{3/2}$ state by an emission at 442.60 nm. For an excitation laser, a tunable laser diode system has been utilized. The laser light is electrically demodulated at 50 kHz by the use of Electro-Optic Modulators (EOM). The fluorescent emission is collected by a fiber optical cable, and then it passes through a 4 nm bandwidth interference filter to reach a high-gain photomultiplier tube (PMT). In order to separate LIF signal from background radiation, fluorescence radiation and electric noise, we employ a First Fourier Transform (FFT) method. In Fig. 5, we show an example of a measured Ion Velocity Distribution Function (IVDF) (parallel component), in the following conditions: P_{rf} of 2,000 W, mass flow rate of 50 sccm and $z = -218$ mm. Here, ion temperature and velocity derived are ~ 0.34 eV and ~ 2.4 km/s, respectively.
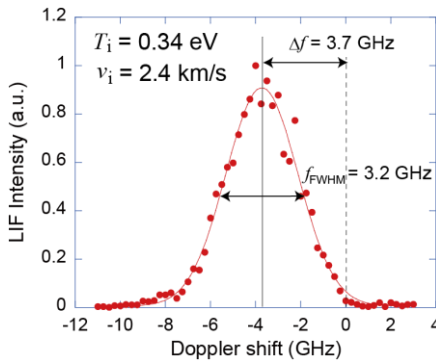

Figure 5. Ion velocity distribution function.

4

III.   Thrust Measurement

In order to measure the thrust produced by an exhaust plasma precisely, a pendulum-type thrust stand with a cylindrical target has been developed. The thrust stand was designed to be capable of measuring impulse bits ranging from 1-100 mN. A basic design is as follows: a large open mouth to collect whole plasma plume, almost no dumping of the target during the measurement time and to withstand ablation by the high-density plasma.
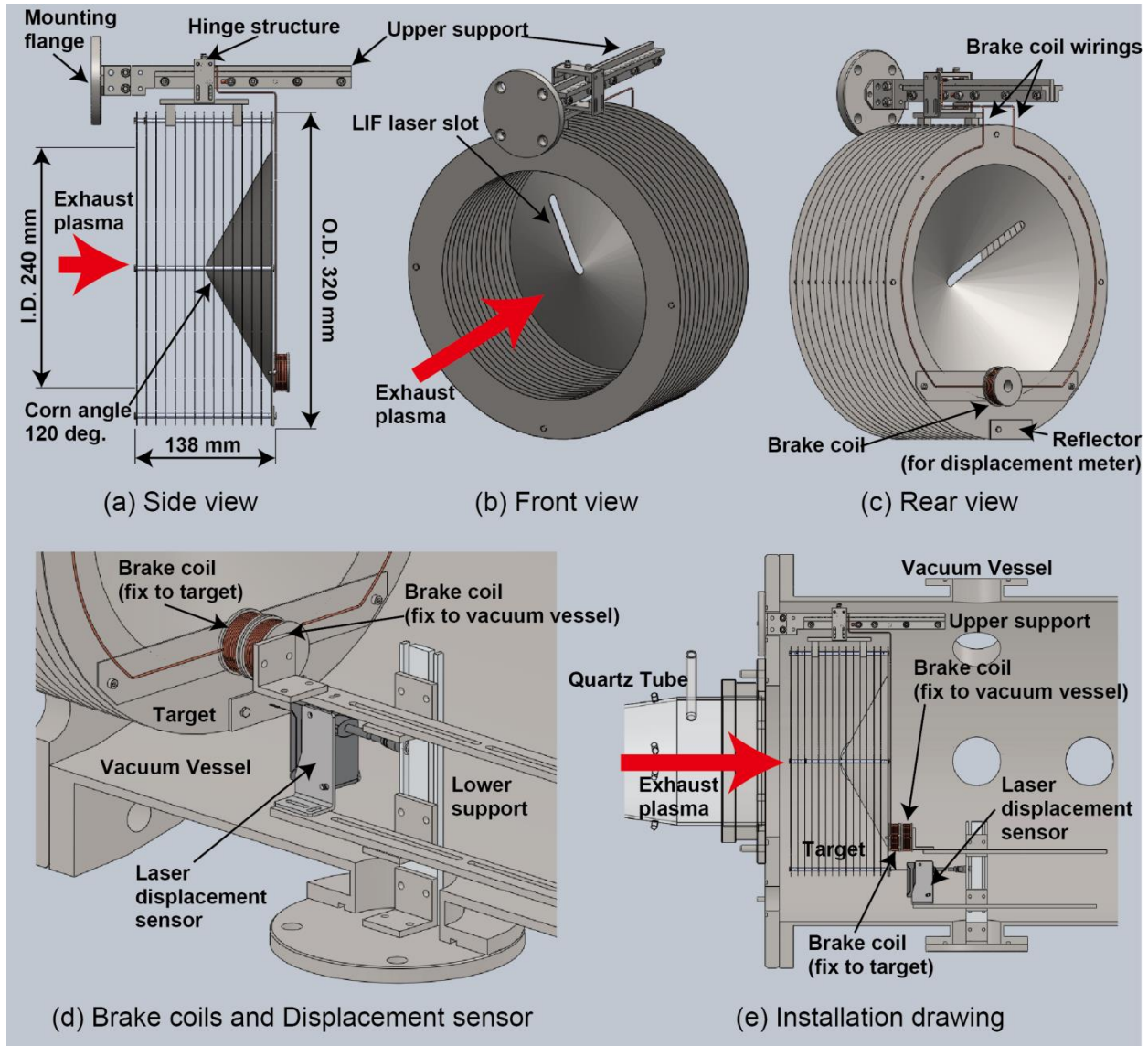

Figure 6. Detail of thrust stand.

Figure 6 shows schematic drawings of the thrust stand, which measures the thrust by a displacement of the target structure using a displacement sensor (IL-S025, Keyence, repeat accuracy: 1 μm). The cylindrical-target is hanged with a quite-low resistance and a low friction by the use of two spikes (target side) and two dimples (upper support side). Since spikes, dimples and the vacuum vessel are insulated each other, the hinge structure can accept target coil current as a completely force-free condition. The target consists of a corn-shape end plate with a 60 degree span from the thruster axis in outer diameter (o.d.) of 320 mm, and a series of 14 thin disks 240 mm with i.d. and o.d. of 320 mm with a thickness of 0.3 mm. The distances between neighboring disks and the end plate are 9.5 mm. Produced ions and neutral particles ejected from the quartz tube enter the target, then collide and reflect by the corn

to the disks directions. At the gap of disks, since particles collide with disks many times, they transfer their axial momentum to the target. Whole structures of target are made of SUS316, with a consideration of a non-magnetization and heat resistance against the high-density plasma. Since the targets was made of SUS316, its weight reaches up to 2 kg. Most thrust stands have a dumping mechanism for the mechanical vibration decay, however in the case of our thrust stand, there is no dumper to keep enough sensitivity against heavy weight. Instead of a passive dumper, this stand has an electromagnetic brake. The electromagnetic brake (shown in Fig. 6(d)) consists of two coils and differential power amplifier. One coil installed at the bottom of the target, another one installed in front of the target coil, it mounted on the vacuum vessel. Currents fed to both two coils are generated by signals from the displacement sensor and differential power amplifier. The magnetic force between two coils stops the target by the negative-feedback. On the other hand, two coils can be utilized as a calibration facility as a well-known force.

Figure 7 shows preliminary results of the thrust measurement. Here, an absolute calibration of thrust has not been done, therefore the value of thrust are shown as arbitrary units. Figure 7(a) shows that the thrust increased with the P_{rf} in all case of gas flow rate. Figure 7(b) shows thrust efficiency, defined as the thrust divided by the input power. In the case of 20 - 50 sccm, this efficiency is increased by increasing of P_{rf}. However, in high mass flow rate cases, e.g., 60 and 70 sccm, the efficiencies were nearly constant. Figure 7(c) shows that the specific impulse increased monotonically due to an increase in the input power.
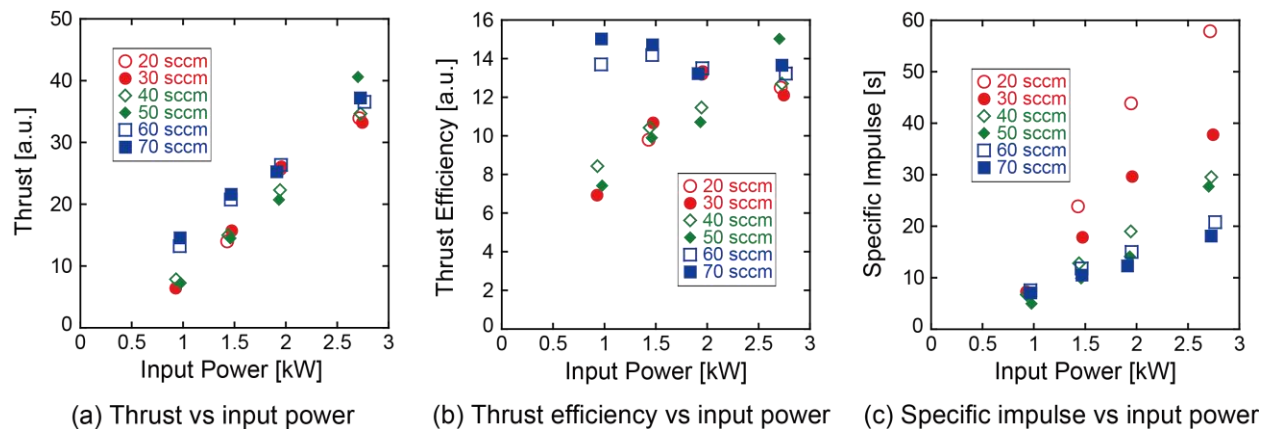

Figure 7. Preliminary result of thrust measurements.

Here, we try to calculate thrust and specific impulse by the use of value without the thrust stand briefly. The thrust is defined as

$$F = n_i m_i v_i^2 \pi r^2 \ [N], \qquad (1)$$

where n_i, m_i and r are, respectively, the ion density, the mass of the ion (Ar) and the radius of plasma. Here, contribution of neutral particles is neglected. According to Langmuir probe and LIF measurements, the typical n_i (average density) and m_i are taken as $\sim 10^{18}$ m^{-3} and 2.4 km/s, respectively using those values with $r = 8.5$ cm, the thrust is calculated to be 8.7 mN. The specific impulse is also calculated by the thrust and mass flow rate, it was determined about 990 s. However, it may be necessary to take account of "backward" mass flow, supplied from open mouth of the quartz cylinder.

IV.   Conclusion

To establish the completely electrodeless helicon plasma thruster, we have been demonstrating experimental acceleration schemes. Using LMD as a discharge facility, a radiofrequency source (7 MHz, ~ 5 kW) produced a high density helicon plasma (> 10^{18} m^{-3}). The acceleration scheme using RMF coils showed the RMF penetration into plasma, and that using $m = 0$ coil showed the change of plasma density. Here, permanent magnets as well as electromagnets were installed to increase B_r for electromagnetic acceleration. In this experiment, various diagnostics system were developed: in addition to Langmuir and Mach probes to obtain n_e and v_i, respectively, spectroscopic measurements have been done using a high-speed camera, a high-resolution monochromator and a diode laser (to deduce the ion velocity distribution function).

The thrust stand developed has an active brake system using two small electromagnets to keep the high sensitivity. As a preliminary result, thrusts were measured under the various input rf power and mass flow rates. Using data by Langmuir and Mach probes, this thrust was estimated briefly. Future works are to determine the calibration of thrust measurements, and a comparison to expected values using measurements of plasma parameters is necessary.

Acknowledgments

References

[1]Shinohara, S., Nishida, H., Tanikawa, T., Hada, T., Funaki, I., Shamrai, K. P., "High-Density Helicon Plasma Sources: Basics and Application to Electrodeless Electric Propulsion," *Transaction of Fusion Science and Technology*, Vol.63, No. 1T, 2013, pp. 164-171.

[2]Boswell, R. W., "Plasma Production using a standing helicon wave," *Physical Letters A*, Vol.33, Issue 7, 1970, pp. 457-458.

[3]Jones, I. R., "A review of rotating magnetic field current drive and the operation of the Rotamak as a field-reversed configuration (Rotamak-FRC) and a spherical tokamak (Rotamak-ST)," *Physics of Plasmas*, Vol. 6 Issue 5, 1999, pp. 1950-1957.

[4]Shinohara, S., Hada, T., Motomura, T., Tanaka, K., Tanikawa, T., Toki, K., Tanaka, Y., Shamrai, K. P. "Development of high-density helicon plasma sources and their application," *Physics of Plasma*, Vol. 16, Issue 5, 2009, pp. 057104-057114.

[5]Shinohara, S., Takechi, S., and Kawai, Y., "Effects of Axial Magnetic Field and Faraday Shield on Characteristics of RF Produced Plasma Using Spiral Antenna," *Japanese Journal of Applied Physics*, Vol. 35, No. 8, 1996, pp. 4503-4508.

[6]Coletti, M., Balestra, A., Sensimi, M., Paccani, G., "Solid State MPD Thruster with Applied Magnetic Field," *Proceedings of the 30th International Electric Propulsion Conference*, University of Roma, Italy, 2007, IEPC-2007-158.

[7]Boivin, R. F., Scime, E. E., "Laser induced fluorescence in Ar and He plasmas with a tunable diode laser," *Review of Scientific Instruments*, Vol. 74, No. 10, 2003, pp. 4352-4360.

[8]Kamio, S., Suzuki, N., Cao, Q. H., Watanabe, G. T., Abe, K., et al., "Development of multi-channel Doppler spectroscopic measurement system using 8x8 multianode photomultiplier tube assembly," *Review of Scientific Instruments*, Vol. 83, Issue 8, 2012, pp. 0831031-0831034.

[9]Boffard, J. B., Jung, R. O., Lin, C. C., Aneskavich, L. E., Wendt, A. E., "Argon 420.1-419.8 nm emission line ratio for measuring plasma effective electron temperature," *Journal of Physics D: Applied Physics*, Vol. 45, 2012, pp. 045201.

[10]Milroy, R. D., "A numerical study of rotating magnetic fields as a current drive for field reversed configurations," *Physics of Plasmas*, Vol. 6, Issue 7, 1999, pp. 2771-2781.

[11]Vlček, J, "A collisional-radiative model applicable to argon discharges over a wide range of conditions. I. Formulation and basic data," *Journal of Physics D: Applied Physics*, Vol. 22, No. 5, 1989, pp. 623-631.